Photogrammetry on 3D Renders of Parametric Built Heritage Models for Interoperability

Etienne Sommer[1], Vasili Manfredi[2], Cecilia Maria Bolognesi[2], Mathieu Koehl[1], Pierre Grussenmeyer[1]

[1]Université de Strasbourg, INSA Strasbourg, CNRS, ICube Laboratory UMR 7357, 67084 Strasbourg, France
(etienne.sommer, mathieu.koehl, pierre.grussenmeyer)@insa-strasbourg.fr
[2] Dept. of Architecture, Built environment and Construction engineering, Politecnico di Milano, 20133 Milano, Italy
(vasili.manfredi, cecilia.bolognesi)@polimi.it

Keywords: Virtual Photogrammetry, 3D Reconstruction, Blender, Low-Poly Mesh, Procedural Rendering, Cultural Heritage.

Abstract

Modelling cultural heritage necessitates the use of specific software and file formats that can be difficult to transpose between one another. These interoperability challenges are particularly acute when employing parametric modelling tools, whether within the context of HBIM or 4D modelling (i.e., the reconstruction of past states of heritage objects). Standard export workflows often fail to preserve complex procedural textures or require time-consuming manual UV unwrapping, rendering direct conversion inefficient. In this study, the potential of applying photogrammetry to synthetic images is investigated as a solution to these limitations. A rigorous dataset is generated in Blender based on a 4D parametric model of a Rhenish castle currently in ruins, utilising path tracing to ensure visual fidelity. This method ensures interoperability by consolidating multiple complex, software-dependent parametric objects into a single, universally compatible mesh. This transformation allows the model to be directly employed across diverse software environments, independent of the original creation tools. Subsequently, the photogrammetric mesh is decimated and optimised to facilitate sharing and viewing on all computer configurations. To validate the approach, a quantitative evaluation is performed: the geometric deviation between the original parametric model and the reconstructed mesh is analysed, and rendering performance is benchmarked to demonstrate the method's suitability for dissemination and visualisation tools.

1. Introduction

The importance of 3D modelling applied to built heritage has been increasingly highlighted in recent years. It provides a digital record of heritage objects, regardless of their size or location, ensuring continuous monitoring while also preserving a digital archive in case of destruction or alteration. Such 3D models can take different forms: on-site surveys using conventional topographic methods (Tsiachta et al., 2024), the use of field data for modelling within an HBIM environment (Rocha et al., 2020), or parametric modelling applicable to various elements of the same type (Parrinello and Pettineo, 2025).

However, in the latter case, significant interoperability issues arise. The resulting models are often optimised for the native software in which they are produced and rely on complex procedural textures or node graphs that fail to translate through standard exchange formats (such as FBX or IFC). Consequently, these assets are not directly usable in other environments without manual conversion.

Beyond conservation, the dissemination of heritage to the public is also a key objective (Innocente et al., 2024). To achieve this, models must be interoperable across different environments and sufficiently optimised to enable sharing on platforms or real-time visualisation (Bolognesi and Manfredi, 2024). In response to this challenge, photogrammetry is applied to synthetic 3D renders of a parametric model of a medieval castle in Alsace, France, created in Blender. This workflow addresses the limitations of standard export methods by consolidating multiple software-dependent parametric objects into a single, unified mesh. This process makes it possible to convert the model into a conventional format optimised for visualisation and dissemination, by drastically reducing the polygon count prior to texturing. Finally, the reliability of this method is assessed through quantitative analysis, specifically regarding geometric deviation and rendering performance.

2. Related Work

Cultural heritage surveys are no longer limited to simple geometry; they now incorporate semantic data, information on state changes, or elements of geometric alteration (Niccolucci et al., 2023). Consequently, the mesh or 3D object is no longer treated as a static representation of the real object at a specific moment. Instead, it is viewed as an entity capable of evolving over time, reflecting changes caused by human activity or environmental factors (Cinquepalmi and Cumo, 2022). To manage this evolution, the static geometry of a standard mesh is insufficient. Tools capable of adapting to the shapes and specific characteristics of heritage elements are therefore required (Murphy et al., 2009). The ability to modify geometry makes it possible to test new hypotheses regarding construction and historical evolution (Christenson, 2025). Although these methods are highly effective, they often suffer from a lack of interoperability or remain specific to proprietary software (Di Donato et al., 2022; Moyano et al., 2022).

To address these challenges, virtual photogrammetry offers a universal solution by shifting the exchange from code to image. It enables the conversion of any complex procedural object into a standardised mesh through the generation of synthetic views (Esmaeili and Thwaites, 2016). This process fixes the state of the parametric model to a defined geometry with controlled precision and has multiple applications (Frommholz, 2019; Rubinstein, 2025), while remaining iterative: a new virtual acquisition can be done after each modification. The interoperability of the resulting meshes depends not only on their format but also on model optimisation to allow manipulation in third-party software (Koehl et al., 2024), ensuring that the necessary data is retained according to the final objective (Banfi, 2017).

3. Methodology

Based on data acquired on-site or available online, a 4D model of the Birkenfels Castle was produced. This model incorporates elements visible in the current ruins, alongside structures that are no longer extant. The latter were reconstructed based on archaeological hypotheses and comparisons with ruins still visible at other similar castles of the region. Each component was modelled using parametric and procedural processes, following the methodology described by Sommer et al. (2025b). This approach enables individual objects to be adapted rapidly, allowing for structural modifications in accordance with feedback from archaeologists specialising in these edifices. Furthermore, this method offers the advantage of being applicable to various types of ruins, thereby covering a wider scope of application.

3.1 Proposed Method for Synthetic Data Acquisition

The parametric modelling method is carried out directly within the Blender software. It notably utilises an instancing system that allows an initial object to be referenced, duplicated, translated, scaled, or rotated without increasing the scene's polygon count. This instancing system is applicable to any type of object, provided that its geometry remains unmodified. For example, altering the position of a single vertex relative to the initial model is not feasible, as this no longer constitutes a reference to the original object, but rather a modification of its geometry. Consequently, the primary advantage of this system is that it enables the creation of complex and dense scenes while maintaining a low polygon count.

On the other hand, a limitation of this method is quickly encountered: as this system is specific to the Blender software, instances cannot be exported directly. It is possible to convert these instances to generate actual geometry, but this introduces a substantial quantity of polygons into the scene, potentially causing the software to terminate unexpectedly. This high polygon count hinders straightforward use in external software. Furthermore, the issue of texturing presents similar challenges. Although texture baking is feasible and capable of automation (Blender enables process automation via a Python API), the individual export of each element with its own texture poses significant problems regarding file management and detail resolution. UV unwrapping and specific dimensions would need to be performed for each object in relation to the detail required for visualisation, to avoid the unnecessary storage of data that offers no subsequent utility.

The virtual photogrammetry method proposed in this article addresses these issues. It enables the consolidation of all elements into a single comprehensive mesh and the application of textures according to a specific Ground Sampling Distance (GSD), depending on the desired level of detail. This GSD is defined using standard methods based on the acquisition distance and virtual camera parameters, such as sensor size, pixel count, and focal length (Luhmann et al., 2023). An icosphere is positioned around the study object so that its vertices serve as locations for each render, similar to the approach employed in a drone survey. The terrain is from the scene prior to this process. This exclusion allows for unrestricted camera placement, facilitating a greater number of convergent views onto the model, while also avoiding the unnecessary processing of vegetation which does not require re-modelling. From this initial configuration, a preliminary set of renders was generated to produce a simplified mesh, serving to verify the reconstruction quality and identify areas lacking sufficient coverage. Consequently, supplementary camera positions were added to target these occluded zones, ensuring that the GSD remained consistent with the global project parameters. This iterative process resulted in a complete dataset of 823 images.

To assess the efficiency of this distribution, a comparison was performed using the 'Plan Mission' tool in Agisoft Metashape (Agisoft Metashape, 2025), which automates camera positioning based on an input mesh. With a comparable GSD of 4.5 mm and a standard image overlap of 70%, the automated tool projected a survey of 737 images in a very similar way to the icosphere. This figure is not significantly lower than the 823 images obtained via the icosphere method, suggesting that the time required to compute a strictly optimised new set offers limited gain. Furthermore, increasing the overlap to 80% caused the projected count to surge to 1,874 images, a number considerably higher than that of the proposed method.

For each position on the icosphere, the camera is oriented towards the model or a specific point of interest. Renders are subsequently generated via path tracing (Sommer et al., 2025a), with all lighting effects such as shadows or reflections removed beforehand to simulate overcast weather conditions with diffuse lighting. The use of path tracing enables the creation of high-quality image renderings and also allows for the correct processing of procedural textures applied to different objects. Figure 1 shows an example of a rendering used in the virtual photogrammetry process.

Figure 1. Example of a rendering in Blender used for virtual photogrammetry

3.2 Orientation via Structure from Motion (SfM) on Synthetic Data

Image orientation and photogrammetric model reconstruction are performed using Metashape. Generally, the use of Ground Control Points (GCPs) within a photogrammetric project enables the referencing and scaling of the model by determining camera positions in three-dimensional space. In the context of this study, the position and rotation of each image are already known, owing to the positioning method described in subsection 3.1. This configuration eliminates the need for GCPs.

The Blender virtual camera was configured to simulate a full-frame camera. Its sensor measures 36 × 24 mm with a resolution of 7680 × 5120 pixels, resulting in a pixel size of $36 \div 7680 = 24 \div 5120 \approx 4.69$ µm. Consequently, the images have a GSD of approximately 4.5 mm. Image orientation was performed using the ”High” setting in Metashape, with positioning accuracy of the images set to 0.00001 metres, the minimum value permitted by the software. This extremely low uncertainty is derived directly from the a priori knowledge of the image positions and rotations. No distortion correction is applied to the images since they were taken using a ”perfect” virtual lens without optical distortions. The results of SfM on these images are shown in figure 2. Once this basis has been established, the 3D reconstruction, mesh optimisation, and quantitative and qualitative analysis of the models are presented in Section 4.

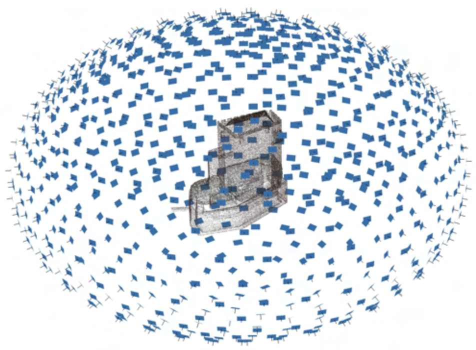

Figure 2. Orientation of the 3D renders in Metashape

4. 3D reconstruction and mesh optimisation

The 3D reconstruction of the virtual photogrammetric model is performed directly within Metashape software. It is generated from depth maps using the ”High” parameter for both quality and face count configuration. The result is a comprehensive mesh of the scene that meets the study’s requirements: all individual parametric objects from the Blender project are consolidated into a single object. Furthermore, the procedural textures of each object are converted into photogrammetric textures applied directly to the mesh. In the subsequent part of the study, a quantitative and qualitative analysis of the photogrammetric mesh is presented. Following this, a mesh decimation process aimed at optimisation is performed and quantified. The mesh optimisation method employed is that proposed by Manfredi et al. (2025).

4.1 Quantitative Analysis of the Photogrammetric Mesh

The quantitative analysis of the reconstruction is performed by comparing the model reconstructed via photogrammetry to the parametric model employed as a case study. This presents a significant advantage: the ground truth can be considered perfect. However, given the complexity of the scene and the topology of the modelled objects, a simultaneous comparison of the entire mesh is not appropriate. Consequently, the analysis focuses on several individual elements of the mesh in relation to the specific objects they represent. It is also important to note that, for this study, no translation is performed between the two models to align them. This facilitates the evaluation of the method’s ability to correctly position the reconstruction in space in the absence of control points, relying only on the known camera positions and rotations.

4.1.1 Study of Surface Planarity The capability of the method to reproduce planar surfaces is assessed by comparing points from the photogrammetric mesh against the reference surface exported from Blender. This comparison is performed within the CloudCompare software utilising the *Cloud/Mesh distance* tool. Signed distances are thereby obtained, as presented in the histogram in figure 3. The distribution of these deviations across the mesh is illustrated in figure 4.

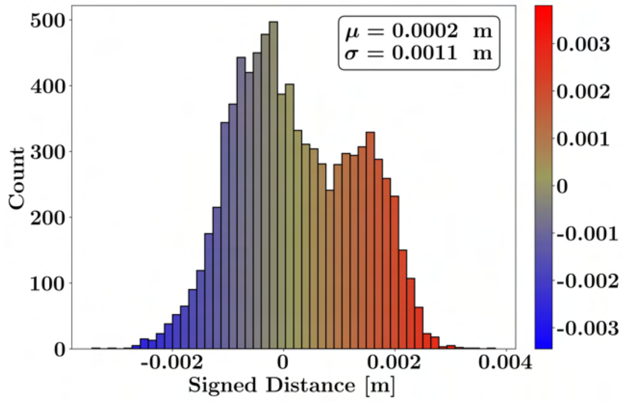

Figure 3. Histogram of signed distances for a planar surface

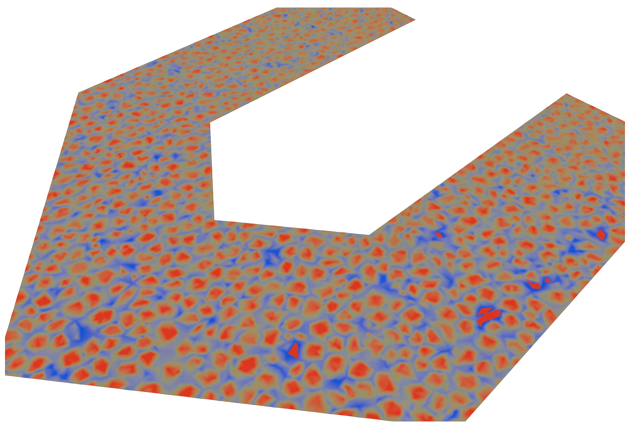

Figure 4. Distribution of deviations on the planar surface
The colour scale is similar to that of figure 3

For 8,735 compared points, the mean distance is 0.2 mm and the standard deviation is 1.1 mm. It is noteworthy that the spatial distribution of these deviations corresponds to the texture applied to the parametric model (a Voronoi-style pattern used to simulate the ground). Based on these results, it is possible to conclude that the method enables the faithful reconstruction of planar surfaces. Should higher accuracy be required, investigating the influence of the parametric mesh’s texture on the capacity to preserve surface planarity would be of interest.

4.1.2 Study of a Complex Surface Composed of Stones of Varying Dimensions Paragraph 4.1.1 demonstrated the method’s capability to reconstruct a planar surface. This section now focuses on the examination of a complex surface. It comprises a collection of stones with varying lengths and heights, each measuring approximately several tens of centimetres. These stones correspond to the bossage masonry typical of Rhenish castles: they feature a convex protrusion of several centimetres at the centre, which contains a lifting hole. Both features are accurately represented in the theoretical model. The histogram in figure 5 presents the distribution of these deviations for 363,574 points, while figure 6 illustrates the spatial distribution of these deviations across the mesh.

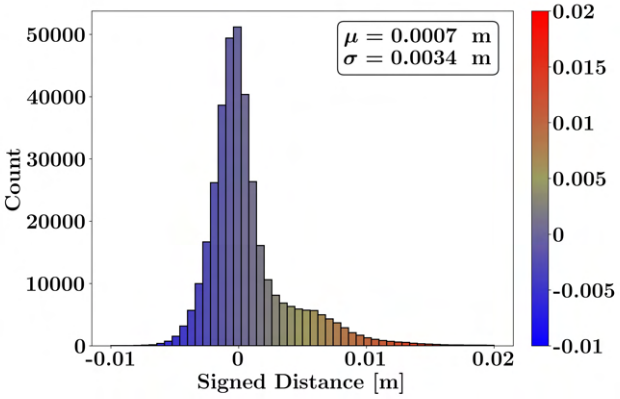

Figure 5. Histogram of signed distances for a complex surface

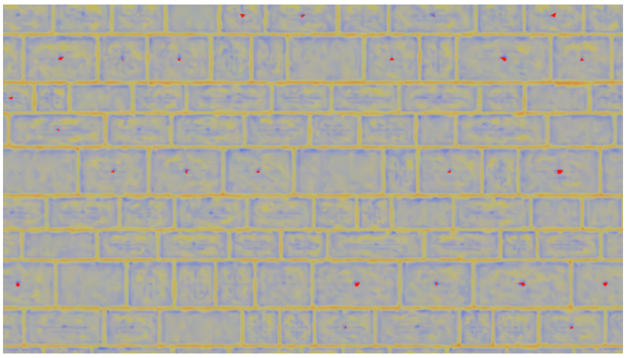

Figure 6. Detail of the stone wall reconstruction deviations. The joints, shown in dark yellow, clearly exhibit larger deviations The colour scale is similar to that of figure 5

It is observed that the mean is approximately 0.7 mm and the standard deviation approximately 3.4 mm, values which are slightly higher than those obtained for the planar surface. Analysis of the location of these deviations reveals that they occur mostly at the surfaces generated to join the individual stones. However, these connecting surfaces do not exist in the reference parametric model, where the stones are positioned adjacently. This identifies the primary source of error: the generation of a continuous surface to connect multiple disjointed elements. Figure 6 highlights this effect. This error is compounded by inaccuracies found at the lifting holes, where the photogrammetric mesh tends to smooth the cavity in comparison to the reference model. These errors remain within the range of a few millimetres and affect only a fraction of the points, leading to the conclusion that the method is capable of reconstructing complex parametric surfaces while effectively merging separate objects. This consolidation enables a drastic optimisation of the geometry, reducing the model complexity from 1,276,458 faces in the original parametric model to 725,026 in the final mesh.

4.1.3 Conclusion of the Quantitative Study of the Photogrammetric Reconstruction Comparisons between the photogrammetric model and the ground truth have demonstrated the method's reconstruction capability. Surface planarity is preserved with millimetric precision, providing a robust foundation for subsequent mesh decimation. Furthermore, complex surfaces can also be faithfully reconstructed. It should be noted that the reconstruction tends to smooth surfaces, potentially resulting in larger deviations in areas of high curvature or when joining distinct objects. Finally, the near-zero mean deviation confirms that the photogrammetric reconstruction, performed without control points, successfully georeferenced the model by relying on the *a priori* known camera positions and rotations. These results extend to other surface types within the model, not presented here for the sake of conciseness.

4.2 Reduction of the Number of Polygons in the Photogrammetric Mesh

The workflow evaluates the decimation method *PixelVR* proposed by Manfredi et al. (2025). The objective is to assess its effectiveness in reducing geometric complexity while preserving visual fidelity for visualisation. Standard optimisation strategies relying on Blender's native architecture, specifically a *legacy* approach using the collapse modifier and a *mixed* strategy incorporating planar decimation, were initially established as comparative baselines. The *legacy* strategy necessitates a segmentation process where boundary vertices must be manually protected to ensure seamless re-joining, while the *mixed* strategy augments this with manual edge collapsing and vertex merging. However, these operator-driven workflows require extensive manual intervention to maintain topological continuity and prevent artefacts. Due to this high dependency on manual oversight and the resulting variability, these native methods were excluded from the primary pipeline in favour of the *PixelVR* solution, which offers a more automated and standardised workflow specifically optimised for real-time constraints.

Prior to optimisation, the dataset underwent a cleaning phase in Blender in order to remove detached or unused polysurfaces, reconstruction noise, and incongruent geometry not belonging to the primary subject. Additionally, operations included the removal of overlapping vertices, coplanar faces, and non-manifold elements, which are the main issues inducing instability during decimation and texture baking.

4.2.1 *PixelVR* Decimation It introduces a procedural, segmentation-aware, and curvature-informed semi-automated workflow in Blender. This approach prioritises reproducibility, scalability, and consistency for large photogrammetric datasets targeting real-time environments. The process starts with model segmentation. Following cleaning, the high-poly mesh is segmented into spatially and topologically coherent parts. Unlike geometric subdivision, this considers structural continuity to reduce local complexity and stabilise optimisation. Concurrently, a curvature-based vertex classification is performed. An analysis evaluates local edge density and geometric variation to identify regions where aggressive decimation would cause perceptual degradation. These vertices are assigned to a protected group excluded from simplification. While not universally linked to perceptual importance, in heritage datasets curvature provides a robust heuristic for preserving carved, ornamented, or organic features. For reduction, the strategy employs a recursive decimation protocol. Instead of a single aggressive pass, a multi-stage process uses predefined presets. Each stage operates on mesh instances, enabling controlled evaluation of optimisation levels. Here, protected vertices remain intact, redundant planar regions are collapsed, and topological checks remove non-manifold edges. This approach reduces the instability of extreme one-pass decimation on dense meshes. Finally, segmented parts are reunited into a unified mesh. Consistent boundary vertices ensure adjacent segments align without visible seams. Coincident vertices are merged, normals recalculated, and scale transformations applied to produce a watertight, engine-ready asset. From the original 6,919,582 faces, the process yielded 281,005 faces, with adaptive density simplifying each section to its specific level of detail. Figures 7 and 8 show the original reconstruction and the final decimated mesh. A colour scale representing face surface area is used to visualise the decimation.

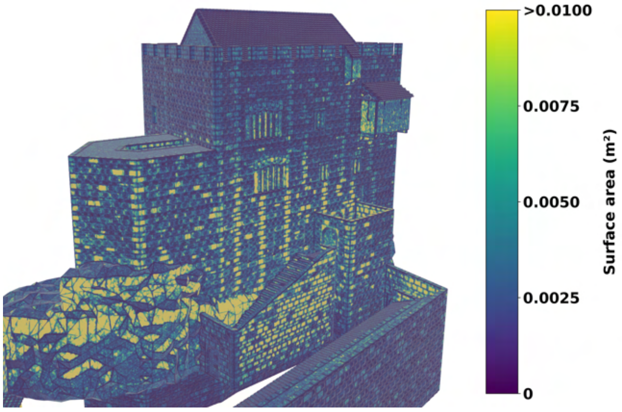

Figure 7. High poly photogrammetric mesh from 3D renders with faces coloured according to their surface area (6,919,582 faces)

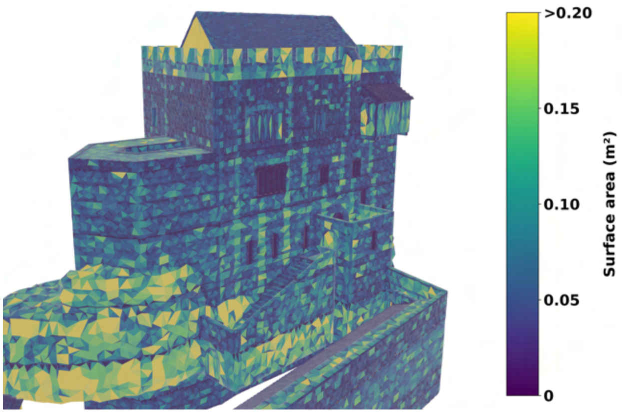

Figure 8. Low poly mesh decimated with *PixelVR* with faces coloured according to their surface area (281,005 faces)

4.2.2 Quantitative Analysis of the Optimised Mesh

Following the same methodology applied to compare the photogrammetric mesh with the initial parametric model, the quality of the decimated model is evaluated using the CloudCompare software. The analysis of the planar surface, previously introduced in section 4.1.1, is not detailed herein. This surface comprises a minimal number of faces that maintain the planarity of the original parametric geometry, rendering further detailed discussion unnecessary. Conversely, it is of greater relevance to examine the effects of decimation on complex surfaces characterised by geometric irregularities. To achieve this, the area selected for analysis corresponds identically to the zone described in section 4.1.2. The histogram illustrating the deviations between the parametric reference and the optimised model is presented in figure 9.

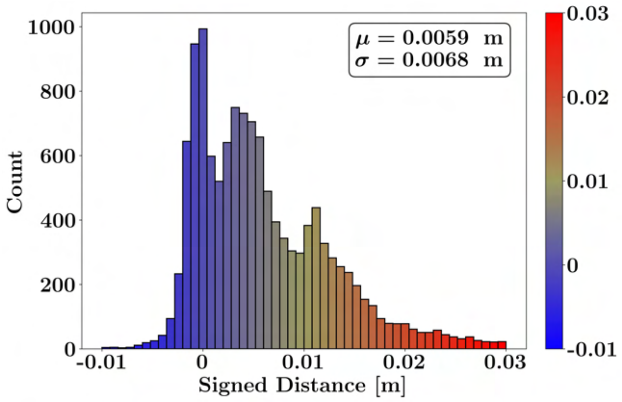

Figure 9. Histogram of signed distances for a complex surface on the optimised mesh

The analysis reveals a mean deviation of approximately 6 mm and a standard deviation of 7 mm. These deviation values are higher than those observed for the initial photogrammetric model. An analysis of the distribution reveals a pronounced asymmetry towards positive values. The vast majority of points are located above zero, indicating a systematic bias wherein the optimised model tends to protrude slightly relative to the reference model. Furthermore, the distribution is not unimodal. It exhibits multiple local peaks, specifically around 0 mm, 5 mm, and 12 mm. This suggests that the error is not random but structural in nature, corresponding to distinct levels of geometric detail, such as the stone surfaces versus the masonry joints, which are processed differently during the simplification stage. These discrepancies can be attributed to the surface approximation process, which inevitably results in a reduction of detail and a divergence from the original geometric features. However, given the calculated metrics, the outcome of the decimation process remains satisfactory, maintaining a close fidelity to the original surface structure.

Furthermore, in contrast to the parametric model, which is composed of multiple distinct elements constructed on an object-by-object basis, it is possible in this case to perform a direct comparison between the entire photogrammetric mesh and the optimised model. While this global approach does not permit a precise, localised analysis of specific surface reconstruction quality, it provides a comprehensive overview of the decimation process across the dataset. Figure 10, which illustrates these geometric deviations, reveals a mean deviation of 1.2 mm and a standard deviation of 4.6 mm. The histogram is characterised by a highly peaked unimodal distribution that is centred approximately on zero. In contrast to the preceding local analysis, no significant secondary peaks are observed in this global dataset. The majority of points are concentrated within a minimal error range, specifically between -2 mm and +5 mm. Although the tails of the distribution extend to several centimetres, they represent a negligible proportion of the total surface area. It can be concluded that the decimation method maintains fidelity to the initial reconstruction, and by extension, to the original parametric model by preserving global coherence despite the significant simplification of the mesh geometry.

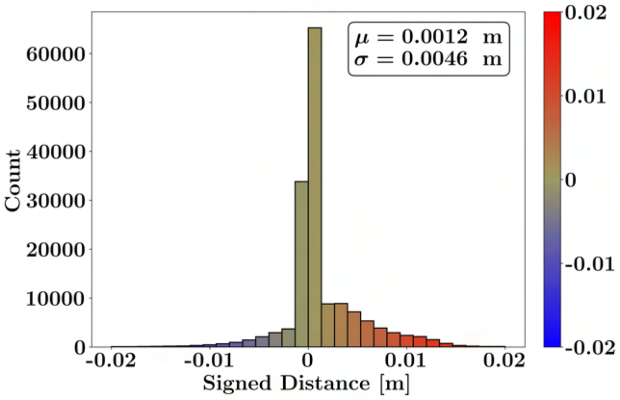

Figure 10. Histogram of signed distances for the entire reconstruction

4.3 Qualitative Analysis of the Conversion from the Parametric Model to the Photogrammetric and Optimised Models

Having established that the photogrammetric reconstruction and its optimisation exhibit minimal deviation from the initial parametric model, the qualitative analysis of the reconstruction enables the determination of whether the result is visually satisfactory in comparison to the initial parametric reference. In the context of this study, the analysis is restricted to a qualitative comparison of the renderings. Mathematical comparison indices exist, such as the Structural Similarity Index (SSIM) score proposed by Wang et al. (2004), but in the present case, a geometric alteration of the model is performed. This transformation could yield SSIM results that are not reflective of rendering quality, but rather biased by the underlying changes in the model's geometric structure.

The geometric details present in the photogrammetric model have been faithfully reconstructed. Edges are sharp, and planar surfaces appear free of noise. Moreover, the geometric optimisation of the model facilitated the smoothing of planar surfaces through face count reduction, whilst retaining sufficient geometry to accurately depict more complex morphological transitions. Additionally, the textures correspond accurately to the level of detail present in the initial images, and they have been correctly mapped onto the model. Originating from procedural textures mathematically generated within Blender using its proprietary node system, the resulting photogrammetric textures enabled the conversion and consolidation of the entire texture set directly onto the unified model. The subsequent baking of these textures ensured the preservation of this level of detail on the optimised model, thereby maintaining visual quality consistency throughout each stage of the processing workflow. Figure 11 presents these results, comparing the wireframe and the rendering for each model.

5. Performance Gain Analysis for Rendering and Visualisation

The geometric and textural optimisation of parametric models offers significant advantages. Primarily, it enhances interoperability between diverse software environments by eliminating dependencies on proprietary parameters inherent to the original modelling tools. Furthermore, it facilitates the manipulation and editing of models, thereby enabling their utilisation on lighter, more portable computing configurations.

Within the context of heritage dissemination, which frames this study, the production of high-quality images and videos is essential for sharing digital assets. However, for complex parametric models, rendering times can extend to tens of minutes or even hours per frame. Reducing this computational burden is therefore critical to enable the generation of substantial volumes of content.

To quantify the efficiency gains achieved through the proposed workflow, a comparative analysis is conducted using path

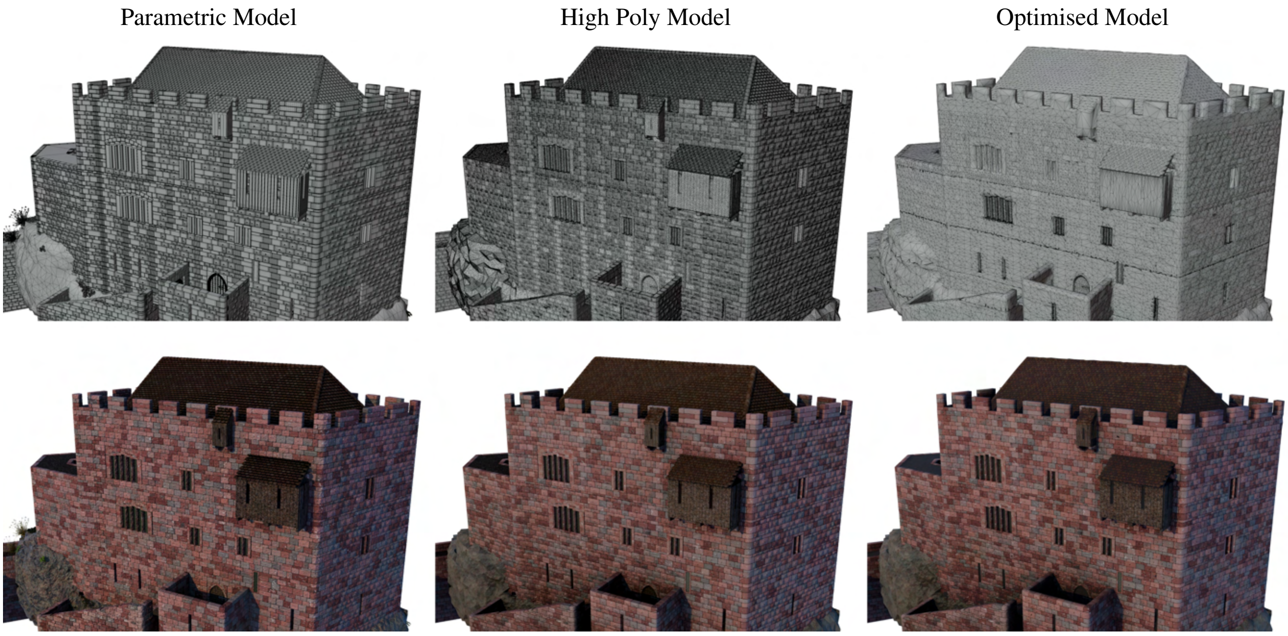

Figure 11. Qualitative comparison of wireframes and textured renders of each model

tracing rendering. This evaluation compares two distinct states of the castle: the reference parametric model and the initial high-poly photogrammetric mesh. For each model, the rendering time per sample is evaluated in order to compare the time savings of the method for generating images from the model. Within the Blender environment, path tracing is the primary method employed to achieve photorealistic results. However, this technique relies on a large number of iterations to reach noise convergence. The rate of this convergence is inversely proportional to the scene's complexity; as the number of elements and their complexity increase, so does the computational burden. By utilising the Blender Python API, the precise duration of individual iterations can be extracted. This allows for a comparative analysis of the total time required to reach a fixed iteration threshold for each model typology. To ensure the validity of these benchmarks, all tests are conducted from a fixed camera viewpoint under identical lighting conditions, provided by a High Dynamic Range Image (HDRI) environment. Additionally, the surrounding terrain is excluded from the scene to strictly isolate the computational load attributable to the castle geometry, preventing vegetation or ground surfaces from biasing the performance metrics. Furthermore, the study is replicated across various resolutions to assess the impact of output size, a decisive factor in determining the perceptibility of fine details. Figure 12 illustrates the temporal evolution of the rendering process across the tested scenarios.

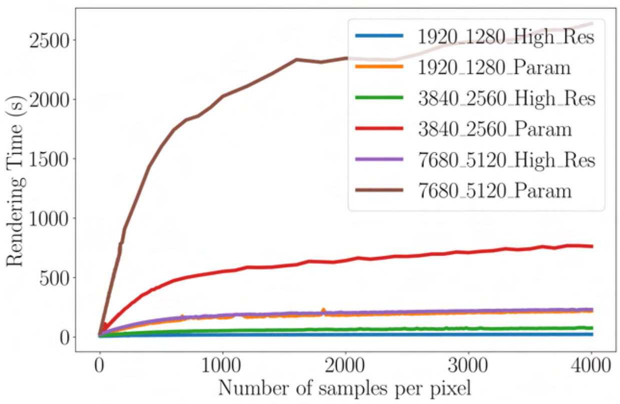

Figure 12. Rendering time for both models at different resolutions

While an increase in resolution logically correlates with extended render times, the data reveals a fundamental disparity in computational behaviour between the two modelling approaches. The parametric model (denoted as 'Param') exhibits a non-linear trajectory, particularly evident at the highest resolution (7680×5120). In this configuration, the computational cost does not scale linearly with the sample count; rather, a sharp initial increase is observed, suggesting a heavy overhead per ray-intersection. This can be attributed to the rendering engine's requirement to dynamically evaluate complex geometry node trees and procedural texture functions for every sample. On the other hand, the model derived from virtual photogrammetry ('High_Res') demonstrates a highly linear and stable progression, regardless of output resolution. The efficiency gap between the two methods is substantial. The baked geometry significantly attenuates the rendering load by converting complex procedural instructions into static mesh data and pre-computed texture maps. Consequently, the path-tracer performs efficient texture lookups rather than resource-intensive procedural mathematical evaluations. This optimisation is quantified by the data: generating imagery at a high resolution of 7680×5120 pixels using the photogrammetric mesh requires approximately the same time as rendering the parametric model at a resolution of 1920×1280 pixels.

6. Conclusion

This study has validated the application of virtual photogrammetry utilising synthetic imagery generated within the Blender software environment. A substantial number of individual parametric objects whose creation is inherently software-specific were successfully consolidated into a single, unified mesh. This resulting geometry is compatible with any standard 3D modelling environment, thereby ensuring significant cross-platform interoperability. Beyond the consolidation of geometric elements, the mathematical procedural textures native to the source software were effectively converted into unified photogrammetric texture maps. This methodology circumvents the requirement for the individual UV unwrapping of each object, as well as the necessity to generate discrete textures for every separate element. It also enables the precise definition of the desired level of detail for texture generation based on virtual camera parameters, thus guaranteeing a consistent resolution and visual homogeneity across the entire model. Finally, it has been demonstrated that, in addition to producing a unified and interoperable asset, this approach yields substantial time savings when utilising the model for subsequent photorealistic rendering tasks.

Several avenues for future research warrant further investigation. In particular, it would be beneficial to establish a more rigorous methodology for defining the optimal positions and orientations of virtual cameras during the virtual photogrammetric survey. Such an optimisation would serve to limit the requisite number of images, thereby streamlining the subsequent photogrammetric processing workflow. Moreover, this method facilitates the creation of models that are readily integrable into applications where performance fluidity is paramount, such as Virtual Reality (VR) environments or online sharing platforms accessible via mobile devices, which typically lack the computational capacity to render excessively complex and voluminous datasets.

Acknowledgement

We extend our thanks to the "Châteaux Rhénans: Burgen am Oberrhein" Interreg VI Project (2023-2025) involving France, Germany, and Switzerland, coordinated by the European Collectivity of Alsace. We appreciate the opportunity to contribute to this innovative approach to digital heritage conservation.

References

Agisoft Metashape, 2025. Agisoft Metashape.

Banfi, F., 2017. BIM Orientation: Grades of Generation and Information for Different Type of Analysis and Management Process. *The International Archives of the Photogrammetry, Remote Sensing and Spatial Information Sciences*, XLII-2/W5, 57–64.

Bolognesi, C. M., Manfredi, V., 2024. Optimization of VR Application in Texturing Cultural Heritage. *The International Archives of the Photogrammetry, Remote Sensing and Spatial Information Sciences*, XLVIII-2/W4-2024, 73–78.

Christenson, M., 2025. Parametric Analysis as a Tool for Hypothesis Generation: A Case Study of the Federal Archive Building in New York City. *Infrastructures*, 10(4).

Cinquepalmi, F., Cumo, F., 2022. Using Digital Twin Models (DTM) for Managing, Protecting and Restoring Historical Buildings. *Conservation Science in Cultural Heritage*, 22(1), 425–445.

Di Donato, D., Morganti, R., Tosone, A., Abita, M., 2022. Procedural Modelling for HBIM of Italian Railways Iron Bridges. *The International Archives of the Photogrammetry, Remote Sensing and Spatial Information Sciences*, XLVI-2/W1-2022, 207–214.

Esmaeili, H., Thwaites, H., 2016. Virtual photogrammetry. *22nd International Conference on Virtual System & Multimedia (VSMM)*, IEEE, Kuala Lumpur, Malaysia, 1–6.

Frommholz, D., 2019. A Synthetic 3d Scene for the Validation of Photogrammetric Algorithms. *The International Archives of the Photogrammetry, Remote Sensing and Spatial Information Sciences*, XLII-2/W13, 1221–1228.

Innocente, C., Nonis, F., Lo Faro, A., Ruggieri, R., Ulrich, L., Vezzetti, E., 2024. A Metaverse Platform for Preserving and Promoting Intangible Cultural Heritage. *Applied Sciences*, 14(8).

Koehl, M., Heitz, J.-E., Sommer, E., Fuchs, M., 2024. Valorization of 3D/4D Models of Disappeared or Ruined Heritage Sites in 3D Modeling Environments. *The International Archives of the Photogrammetry, Remote Sensing and Spatial Information Sciences*, XLVIII-2/W8-2024, 235–242.

Luhmann, T., Robson, S., Kyle, S., Boehm, J., 2023. *Close-Range Photogrammetry and 3D Imaging*. De Gruyter, Berlin, Boston.

Manfredi, V., Bolognesi, C. M., Fai, S., 2025. PIXEL VR: Optimizing Photogrammetric Datasets for Standalone VR. *The International Archives of the Photogrammetry, Remote Sensing and Spatial Information Sciences*, XLVIII-M-9-2025, 973–980.

Moyano, J., Carreño, E., Nieto-Julián, J. E., Gil-Arizón, I., Bruno, S., 2022. Systematic Approach to Generate Historical Building Information Modelling (HBIM) in Architectural Restoration Project. *Automation in Construction*, 143, 104551.

Murphy, M., McGovern, E., Pavia, S., 2009. Historic Building Information Modelling (HBIM). *Structural Survey*, 27(4), 311–327.

Niccolucci, F., Markhoff, B., Theodoridou, M., Felicetti, A., Hermon, S., 2023. The Heritage Digital Twin: A Bicycle Made for Two. The Integration of Digital Methodologies into Cultural Heritage Research. *Open Research Europe*, 3(64).

Parrinello, S., Pettineo, A., 2025. Databases and Information Models for Semantic and Evolutionary Analysis in Fortified Cultural Heritage. *Heritage*, 8(1).

Rocha, G., Mateus, L., Fernández, J., Ferreira, V., 2020. A Scan-to-BIM Methodology Applied to Heritage Buildings. *Heritage*, 3(1), 47–67.

Rubinstein, J., 2025. [DC] Exploring virtual photogrammetry techniques and applications for advancement of digital twin generation. *IEEE Conference on Virtual Reality and 3D User Interfaces Abstracts and Workshops (VRW)*, IEEE, Saint Malo, France, 1550–1551.

Sommer, E., Koehl, M., Grussenmeyer, P., 2025a. Comparative Study of Path Tracing Rendering Parameters and Visual Quality in Blender. *The International Archives of the Photogrammetry, Remote Sensing and Spatial Information Sciences*, XLVIII-M-9-2025, 1387–1394.

Sommer, E., Koehl, M., Grussenmeyer, P., 2025b. Parametric Modelling Techniques for Rhine Castle Models in Blender. *Heritage*, 8(1).

Tsiachta, A., Argyrou, P., Tsougas, I., Kladou, M., Ravanidis, P., Kaimaris, D., Georgiadis, C., Georgoula, O., Patias, P., 2024. Multi-Sensor Image and Range-Based Techniques for the Geometric Documentation and the Photorealistic 3D Modeling of Complex Architectural Monuments. *Sensors*, 24(9), 2671.

Wang, Z., Bovik, A., Sheikh, H., Simoncelli, E., 2004. Image Quality Assessment: From Error Visibility to Structural Similarity. *IEEE Transactions on Image Processing*, 13(4), 600–612.